Journal of Inorganic Biochemistry 102 (2008) 2052–2059

Contents lists available at ScienceDirect

Journal of Inorganic Biochemistry

journal homepage: www.elsevier.com/locate/jinorgbio

DNA binding and bending by dinuclear complexes comprising ruthenium polypyridyl centres linked by a bis(pyridylimine) ligand

Ursula McDonnell [a], Matthew R. Hicks [a], Michael J. Hannon [b,1], Alison Rodger [a,*]

[a] Department of Chemistry, University of Warwick, Coventry CV4 7AL, UK
[b] School of Chemistry, University of Birmingham, Edgbaston, Birmingham B15 2TT, UK

ARTICLE INFO

Article history:
Received 9 March 2008
Received in revised form 3 June 2008
Accepted 3 June 2008
Available online 20 June 2008

Keywords:
Bimetallo complexes
Ruthenium metal complexes
DNA binding
Linear dichroism
DNA bending

ABSTRACT

The interaction of enantiomerically pure dinuclear complexes of the form $[Ru_2(L–L)_4L^1]^{4+}$ (where L–L = 2,2′-bipyridine (bpy) or 1,10-phenanthroline (phen) and L^1 = bis(pyridylimine) ligand ($(C_5H_4N)C{=}N(C_6H_4))_2CH_2$)) with ct-DNA have been investigated by absorbance, circular dichroism, fluorescence displacement assays, thermal analysis, linear dichroism and gel electrophoresis. The complexes all bind more strongly to DNA than ethidium bromide, stabilise DNA and have a significant bending effect on DNA. The data for Δ,Δ-$[Ru_2(bpy)_4L^1]^{4+}$ are consistent with it binding to DNA outside the grooves wrapping the DNA about it. By way of contrast the other complexes are groove-binders. The phen complexes provide a chemically and enantiomerically stable alternative to the DNA-coiling di-iron triple-helical cylinder previously studied. In contrast to the di-iron helicates, the phen complexes show DNA sequence effects with Δ,Δ-$[Ru_2(phen)_4L^1]^{4+}$ binding preferentially to GC and Λ,Λ-$[Ru_2(phen)_4L^1]^{4+}$ to AT.

1. Introduction

Ruthenium polypyridyl complexes have applications in the fields of biochemistry, photochemistry and photophysics [1–8]. The last few decades have seen an increased interest in ruthenium(II) polypyridyl complexes as building blocks in supramolecular devices due to their favourable excited state and redox properties as well as structural probes for DNA [9–14]. Ruthenium complexes are also showing promising results in anti-tumor activity and they target a broad spectrum of cancers [15–20].

The most investigated mononuclear polypyridyl ruthenium complexes are the ruthenium tris(chelates), $[Ru(bpy)_3]^{2+}$ (bpy = 2,2′-bipyridyl) and $[Ru(phen)_3]^{2+}$(phen = 1,10-phenanthroline). The bipyridine and phenanthroline ligands are coordinated to the octahedral metal centre and are shaped like three-bladed propellers resulting in the enantiomers corresponding to right and left handed screws, denoted Δ or P and Λ or M, respectively. The binding modes of $[Ru(phen)_3]^{2+}$ to DNA have been disputed in literature for several years; however, there is general agreement that $[Ru(phen)_3]^{2+}$ displays enantiomeric selectivity in binding to DNA [11,12,21–25]. The mononuclear ruthenium(II) complexes span only 1–2 DNA base pairs and are easily displaced from DNA at low ionic strengths [26]. A number of dinuclear complexes have been reported in the literature and as they have increased in size, shape and charge they show a greater DNA binding affinity and are generating much interest as probes for DNA [27]. Dinuclear complexes possessing two $[Ru(phen)_2dppz]^{2+}$ (dppz = dipyrido[3,2-a:2′,3′-c]phenazine) units linked together using a bridging ligand have been shown to form a bis(intercalating) metallo complex [28]. Other dinuclear bis(intercalator)s include complexes of the form $[\{Ru(dpq)_2\}_2(phen\text{-}x\text{-}SOS\text{-}x\text{-}phen)]^{4+}$ which bind to DNA via the dpq ligand, (dpq = dipyrido[3,2-d:2′3′-f]quinoxaline; SOS = 2-mercaptoethyl ether; x = 3, 4 or 5) [13,26]. Different binding affinities and site sizes can be achieved by systematically varying the linker and its point of attachment. The bridged dinuclear ruthenium complex $[\{Ru(Me_2bpy)_2\}_2(\mu\text{-bpm})]^{4+}$ (bpm = 2,2′-bipyrimidine) binds strongly to open structures such as partially denatured DNA [29].

In contrast to the literature, our work on dinuclear ruthenium compounds has been targeted at groove-binders which could span ~5 base pairs and have increased charge compared with the mononuclear complexes. The starting point for our design was the di-iron triple helicate cylinders of Fig. 1. This parent compound is tetracationic and has demonstrated strong non-covalent binding to DNA with exciting possibilities for structural control of DNA. When added to genomic or other long DNA, it intramolecularly coils up DNA [30–33], and when added to short palindromic oligonucleotides with AT-rich central sequences [34] it recognises or creates a three-way junction from three DNA oligonucleotides. Because of these exciting and unprecedented DNA binding properties we were intrigued to explore the effects on DNA of compounds

* Corresponding author. Fax: +44 2476 524112/+44 2476 575795.
E-mail addresses: m.j.hannon@bham.ac.uk (M.J. Hannon), a.rodger@warwick.ac.uk (A. Rodger).
[1] Fax: +44 121 414 7871.

0162-0134/$ - see front matter © 2008 Elsevier Inc. All rights reserved.
doi:10.1016/j.jinorgbio.2008.06.006

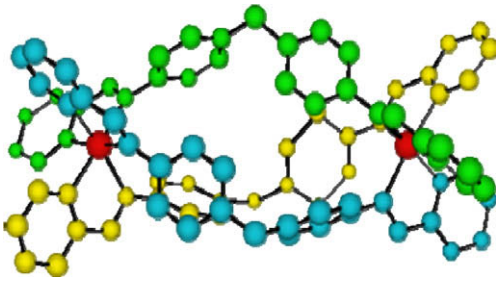

Fig. 1. Structure of the iron triple-helical cylinder, $[Fe_2L^1_3]^{4+}$, where $L^1 = C_{25}H_{20}N_4$ a bis(pyridylimine) ligand containing a diphenylmethane spacer.

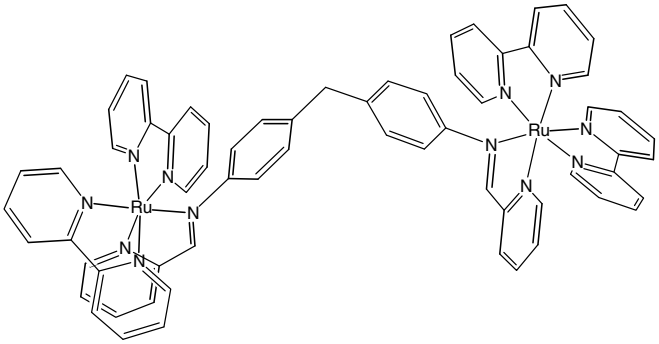

Fig. 2. $[Ru_2(bpy)_4L^1]^{4+}$.

with related structures. Complexes based on ruthenium are particularly attractive because of their photochemical properties and their high kinetic stability towards racemisation and ligand exchange. However, this stability towards ligand exchange reactions does complicate the synthesis: the ruthenium triple-stranded cylinder can be prepared [6] but not in a high yielding supramolecular self-assembly reaction [30,31,34,35,38] as used to make the di-iron cylinder. The focus herein was the design of alternate ruthenium(II) compounds of type illustrated in Fig. 2 where two ruthenium bis(chelates) have been linked into one unit with a single bis(pyridylimine) linker ligand common to both metals [38]. The synthesis and characterisation of the diruthenium bipyridine complex $[Ru_2(bpy)_4L^1]^{4+}$ and its phenanthroline analogue $[Ru_2(phen)_4L^1]^{4+}$ are reported in Ref. [38]. Enantiopure $[Ru(LL)Cl_2]$ starting materials afforded the homochiral ΔΔ and ΛΛ enantiopure products. In structure, these dinuclear metal complexes are each part way between being two stacked monoruthenium tris(chelates) (so might bind in the high loading modes of such complexes) [23] and a less symmetric version of the di-iron cylinder. In this paper, we report their DNA binding.

2. Materials and methods

2.1. Chemicals

All reagents and solvents were purchased commercially and used without further purification unless otherwise stated. Ultrapure water (18.2 Ω) was used in all experiments. Calf thymus DNA (ct-DNA, Type 1 highly polymerised sodium salt form) was purchased from Sigma-Aldrich Chemical Co. Ltd. The synthetic double-stranded DNA copolymers, poly[d(A–T)$_2$] and poly[d(G–C)$_2$], were purchased from Amersham Biosciences. Plasmid DNA pBR322 was purchased from New England Biolabs. All polynucleotides were dissolved in water (ct-DNA requiring overnight refrigeration to become solubilised) and frozen until the day of the experiment. The concentrations (bases per litre) of the DNA solutions were determined spectroscopically using the molar extinction coefficients: ct-DNA $\varepsilon_{258} = 6600\ M^{-1}\ cm^{-1}$; poly[d(A–T)$_2$] $\varepsilon_{262} = 6600\ M^{-1}\ cm^{-1}$; poly[d(G–C)$_2$] $\varepsilon_{254} = 8400\ M^{-1}\ cm^{-1}$. The concentration of pBR322 as supplied was 1000 μg/ml. Fifty millilitres of 0.2 M sodium cacodylate (4.28 g of Na $(CH_3)_2AsO_2 \cdot 3H_2O$ in 100 ml) was mixed with 9.3 ml; of 0.2 M hydrochloric acid and diluted to 200 ml with water to make 100 mM sodium cacodylate buffer, pH = 7.0. (Δ,Δ)-$[Ru_2(bpy)_4L^1](PF_6)_4$ (referred to as (P)-bpy herein) [36,37]; (Λ,Λ)-$[Ru_2(bpy)_4L^1](PF_6)_4$ (referred to as (M)-bpy); (Δ,Δ)-$[Ru_2(phen)_4L^1](PF_6)_4$ (referred to as (P)-phen); (Λ,Λ)-$[Ru_2(phen)_4L^1](PF_6)_4$ (referred to as (M)-phen) and their diastereomeric mixtures were prepared as described previously [38]. $[Fe_2L^1_3]^{4+}$ was prepared according to our previously described proceedures [30,31,36,40]. The ruthenium complex concentrations were determined by weight and the iron complexes concentrations were determined using UV/visible absorbance spectroscopy and the extinction coefficient $\varepsilon_{574\ nm} = 16{,}900\ M^{-1}\ mol^{-1}$[41].

2.2. Absorbance and circular dichroism spectroscopy

One solution containing: DNA (1500 μM), NaCl (50 mM), sodium cacodylate buffer (1 mM) and metal complex (15 μM) and a second solution containing NaCl (50 mM), sodium cacodylate buffer (1 mM) and metal complex (15 μM) were prepared. The first spectrum measured was of the DNA–metal complex solution. By adding increasing volumes of the second DNA-free solution to the cuvette, the concentration of DNA was decreased whilst the metal complex, NaCl and sodium cacodylate buffer concentrations remained constant. UV/visible absorbance spectra were collected on a Jasco V-550 and CD spectra were collected on a Jasco J-715 spectropolarimeter. A water baseline was subtracted from each data set.

2.3. Fluorescence competition binding assay

A solution of DNA (12 μM), NaCl (50 mM), buffer (1 mM) and ethidium bromide (EB, 15 μM) was prepared. The ruthenium complex concentration was incrementally increased from EB:metal complex ratios of 200:1 to 1:1 while keeping the concentrations of DNA and EB constant. Fluorescence spectra were collected at each ratio on a Perkin Elmier LS50B fluorimeter with excitation at 540 nm, excitation slit 10.0 and emission slit 15.0 nm.

2.4. Thermal analysis

The stability of DNA in the presence of the bimetallo complexes was monitored by measuring the absorbance at 260 nm (1 nm bandwidth, average time: 10 s, ramp rate 0.5 °C/min) as a function of temperature. The experiment was run simultaneously on six masked 1 cm pathlength cuvettes of 1.2 ml volume using a Peltier controlled 6-sample cell-changer in a Cary 1E spectrophotometer. One DNA, and five DNA–metal complex solutions of different DNA:complex ratios were prepared for each run. T_m was calculated by smoothing the data over 20 data points and numerically differentiating using Kaleidagraph.

2.5. Flow linear dichroism

A flow linear dichroism (LD) titration series was carried out using a Jasco J-715 spectropolarimeter adapted for LD spectroscopy whilst keeping the DNA concentration constant at 200 μM. A large volume Couette flow LD cell built by Crystal Precision Optics, Rugby (now available from Dioptica Scientific Ltd.) based on the design described in [42] was used in all experiments. One solution containing: DNA (200 μM), NaCl (50 mM) and sodium cacodylate buffer (1 mM) and a second solution containing: DNA (400 μM), metal

complex, NaCl (50 mM) and sodium cacodylate buffer (1 mM) were prepared. By adding equal volumes of the concentrated DNA and the DNA/metal complex solutions to the flow cell, the concentration of DNA, NaCl and sodium cacodylate remained constant while the DNA:metal complex ratio decreased.

2.6. Gels electrophoresis

Gel electrophoresis experiments were carried out using an Amersham HE99X Max Submarine Unit, powered by an Amersham EPS 3051 XL Power Unit. Gel trays of 100 × 200 mm were used; a tooth comb was used to produce sample wells 5 mm deep. 1× tris–acetate EDTA (1× TAE) running buffer (Fisher Scientific, Loughborough, UK) was used [43]. Agarose powder was mixed with the electrophoresis buffer to the desired concentration, 1% (w/w). Sixteen microliters of the samples were loaded into the wells and a current of 130 V was applied. All samples were run in 1× DNA loading buffer (Bioline, London, UK) [43]. The samples were stained with ethidium bromide for 15–20 min, visualised under a UV lamp and photographed using a UV/vis transilluminator Uvidoc from Uvitec.

3. Results and discussions

The interaction of the dimetallo ruthenium complexes with DNA was probed by a combination of biophysical techniques as outlined below.

3.1. Absorbance spectroscopy

The absorbance spectra of aqueous solutions of the linker ligand L^1, $[Ru_2(bpy)_4L^1]^{4+}$ and $[Ru_2(phen)_4L^1]^{4+}$ are overlaid in Fig. 3. The linker metal ligand charge transfer (MLCT) spectroscopy is found at 400–500 nm and includes the pyridylimine and phen/bpy MLCT transitions. Ligand-based transitions are found at lower wavelength [11,12,23,39]. Upon interaction of the metal complexes with ct-DNA changes in magnitudes and shifts in wavelength maxima relative to the free metal complex were observed, indicative of an association with DNA (data not shown) [23,44,45].

3.2. CD spectroscopy

The CD spectra of aqueous solutions of the enantiomers of $[Ru_2(bpy)_4L^1]^{4+}$ and $[Ru_2(phen)_4L^1]^{4+}$ are shown in Fig. 4. When ct-DNA is added to the complexes, their CD spectra change as shown by the non-zero ICD (induced CD) of the enantiomers (Fig. 5, MLCT region, and Supplementary information Figure S1, DNA region).

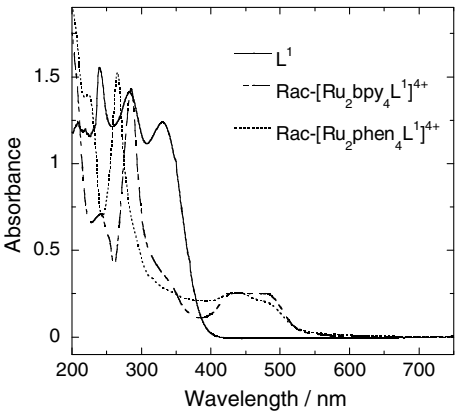

Fig. 3. Absorbance spectra of aqueous solutions (20 μM, 1 cm pathlength) of $[Ru_2(bpy)_4L^1]^{4+}$, $[Ru_2(phen)_4L^1]^{4+}$ and L^1.

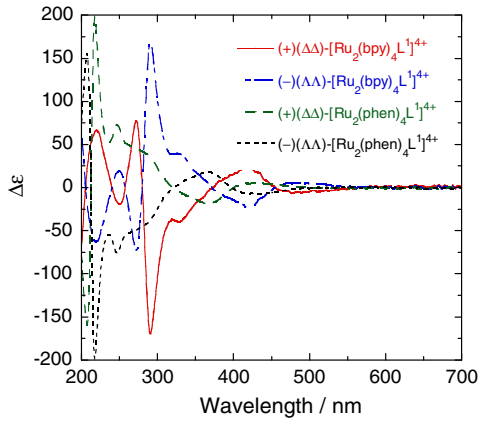

Fig. 4. CD spectra of aqueous solutions of (P)- and (M)-$[Ru_2(bpy)_4L^1]^{4+}$ (15 μM) and (b) (P)- and (M)-$[Ru_2(phen)_4L^1]^{4+}$ (15 μM)) plotted as $\Delta\varepsilon$. Spectra were collected in a 1 cm pathlength cell.

(P)-bpy has little ICD at 500 nm and a negative signal at 400 nm with no change in ICD as DNA concentration is reduced. This means that there is no change in binding mode as the DNA concentration is reduced suggesting that the binding to different DNA sequences has the same strength so there is no change in sequence occupied as the loading increases. (M)-bpy, (P)-phen and (M)-phen by way of contrast, all show a decrease in CD intensity and a change in shape as the DNA concentration is reduced. Their high binding constants (see below) would suggest this is due to a combination of sequence dependence of the binding and possibly a change in binding mode. In each case, both the MLCT region and DNA region spectral changes are linear with DNA concentration (*i.e.* mixing ratio) at low loading. The DNA region pBR322 plasmid ICD spectra are shown in Supplementary Figure S2. For each complex the overall features are similar for ct-DNA and the plasmid suggesting that the binding modes with ct-DNA and the plasmid used in the gel electrophoresis experiments (see below) are similar.

3.3. Fluorescence competitive binding studies

An ethidium bromide (EB) competition assay was carried out for each complex with the concentrations of DNA and EB kept constant as more ruthenium complex was added to the solution. As the ruthenium complex was added, the ethidium bromide fluorescence decreased (Fig. 6). This might be due either to the metal complex competing with EB for the binding sites on the DNA thus displacing the EB (whose fluorescence is enhanced upon DNA binding) or it could be a more direct quenching interaction on the DNA itself. We assume it is the former which implies that all the complexes bind more strongly to DNA than EB at 50 mM NaCl concentration. A qualitative ranking of the DNA binding strength of both the bpy and phen complexes is: (M) > diastereomeric mixture > (P) with the bpy all binding less strongly than the phen complexes. The DNA binding constant of EB at 50 mM NaCl was taken to be $\sim 1.2 \times 10^6\ M^{-1}$ [46] from which the binding constants of Table 1 were determined using the method of Ref. [46]. The ability of the complexes to displace EB is lower than that of the iron(II) tetracationic cylinders of L^1 but significantly higher than that of related mononuclear ruthenium polypyridyl complexes [11,12,23]. The values of K for the diruthenium complexes of this work are sufficiently large that we can conclude that in the experiments reported herein essentially all the metal complex added to the DNA solutions is bound to DNA.

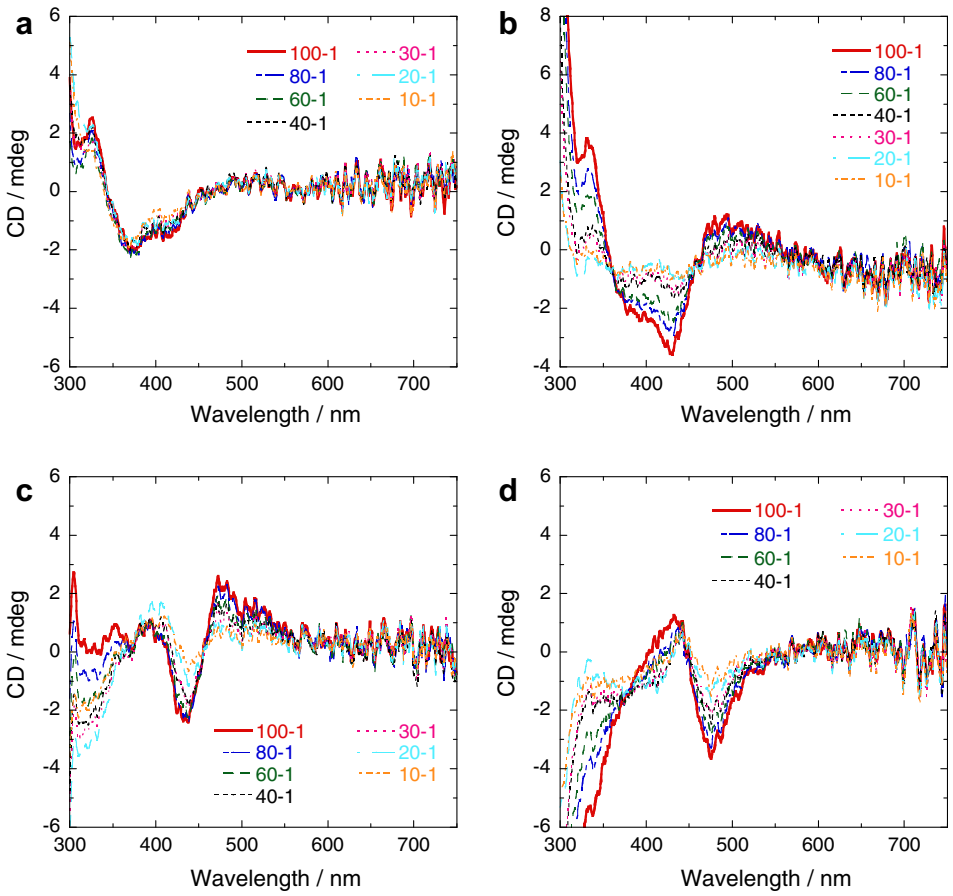

Fig. 5. ICD spectra (obtained by subtracting the free metal complex spectra from the ct-DNA plus metal complex CD spectra) spectra for constant complex concentration (15 μM) and varying ct-DNA concentrations. (a) (P)-$[Ru_2(bpy)_4L^1]^{4+}$, (b) (M)-$[Ru_2(bpy)_4L^1]^{4+}$, (c) (P)-$[Ru_2(phen)_4L^1]^{4+}$ and (d) (M)-$[Ru_2(phen)_4L^1]^{4+}$. Mixing are ratios indicated in each figure. All spectra were run in 50 mM NaCl and 1 mM sodium cacodylate buffer with 18.2 MΩ water. The cell path length was 1 cm.

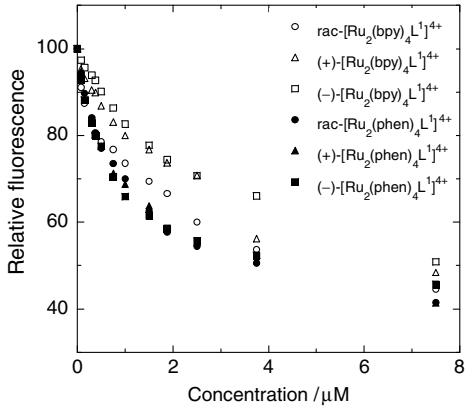

Fig. 6. Fluorescence intensity at different concentrations of $[Ru_2(bpy)_4L^1]^{4+}$ and $[Ru_2(phen)_4L^1]^{4+}$ with constant DNA (12 μM) and EB (15 μM) concentration. Data are averaged over 9 data points (588–592 nm) and normalised to a starting intensity of 100. All spectra were run in 50 mM NaCl and 1 mM sodium cacodylate buffer with 18.2 MΩ water. The cell pathlength was 1 cm. Rac refers to the diastereomers.

3.4. Thermal analysis

The melting curves of ct-DNA in the presence of different ruthenium complexes were investigated to show whether the metal complex interaction with ct-DNA causes a thermal stabilising or destabilising effect on the DNA duplex. The melting curves and the first derivative plots for the reactions are given in Supplementary information (Figures S3 and S4). In all cases T_m increased from the ct-DNA value of 73.0° by 2–3° which is characteristic of a non-intercalative binding mode. The stabilisation of the DNA duplex increases as the amount of added ruthenium complex increases. In accord with their binding constants, the phen complexes stabilise the DNA by ~3 °C and the bpy by ~2 °C. However, there is an inverse correlation between the binding constants and the increasing T_m values within each set of complexes suggesting that the complexes with the larger binding constants reduce backbone–backbone repulsion less effectively. The increase in T_m is in each case much less than that induced by the major-groove binding and DNA-coiling iron(II) cylinders [31].

3.5. Linear dichroism

As noted above we were interested to see whether the diruthenium complexes behaved as two stacked metal tris(chelates) (thus, the high loading monoruthenium complex binding modes) or as the dimetallo iron(II) cylinders. LD is the ideal tool to probe both changes in ligand orientation as a function of loading and DNA bending. LD titration series were, therefore, carried out keeping the DNA concentration constant at 200 μM.

A decrease in the DNA signal intensity at 260 nm was observed upon addition of each complex (Fig. 7), indicating a decrease in the orientation of the DNA such as is associated with bending or coiling of the DNA but could also be an increase in flexibility. As summarised in Table 1, at 30:1 loading the (P) and (M)-complexes have

Table 1
Summary of DNA interactions of the bis(ruthenium) complexes compared with $[Fe_2L^1_3]^{4+}$ complexes

EB displacement	(P)-bpy	Diastereomeric-bpy	(M)-bpy	(P)-phen	Diastereomeric-phen	(M)-phen	(P)-Fe_2	Rac-Fe_2	(M)-Fe_2
	Least					Most	Least		Most
$K_h/(10^6\ M^{-1}) \pm 10\%$	5.1	11	12	17	25	36	70[40]	60[40]	70[40]
ΔT_m (°C) at 30:1 DNA:complex	+3.0	+2.6	+1.9	+3.8	+3.6	+3.4			
ct-DNA ICD as a function of *r*	Constant	~0	Changes	Changes	~0	Changes			
ICD sign pattern 500 nm/430 nm/380 nm	0/−/−	Small 0/−/−	+/−/−	+/−/+	Small 0/−/−	−/+/0			
% Loss in LD ct-DNA at 30:1 DNA:complex	20	2	19	17	7	16	43[30]@50:1 20 mM NaCl	85[29]@50:1 20 mM NaCl	95[30]@50:1 20 mM NaCl
% Loss in LD GC-DNA at 30:1 DNA:complex	7	20	6	46	41	50			
% Loss in LD AT-DNA at 30:1 DNA:complex	46	49	26	36	29	91			
MLCT LD magnitude and sign ct-DNA	Small −ve/+ve	~0	Large +ve	Large +ve	~0	Small +ve	Large (P)	Small (P)	Small (P)
MLCT LD magnitude and sign AT-DNA	~0	~0	~0	Large +ve	~0	~0			
MLCT LD magnitude and sign GC-DNA	~0	~0	~0	~0	~0	~0			
Slowing of gel migration (arbitrary scale)	~0	1	2	2	1	3		4	

All ruthenium solutions were: 50 mM NaCl and 1 mM sodium cacodylate buffer.

the same bending or coiling effect on the DNA. However, the coiling is much less than that induced by the di-iron(II) cylinders where the more effective M enantiomer has induced a 66% loss of orientation at 50:1 loading [30,31]. The diastereomeric mixtures are significantly less effective at bending DNA (data summarised in Table 1), suggesting that in each case the components of the diastereomeric mixtures have opposing bending effects when all are present since the complexes have strong binding constants.

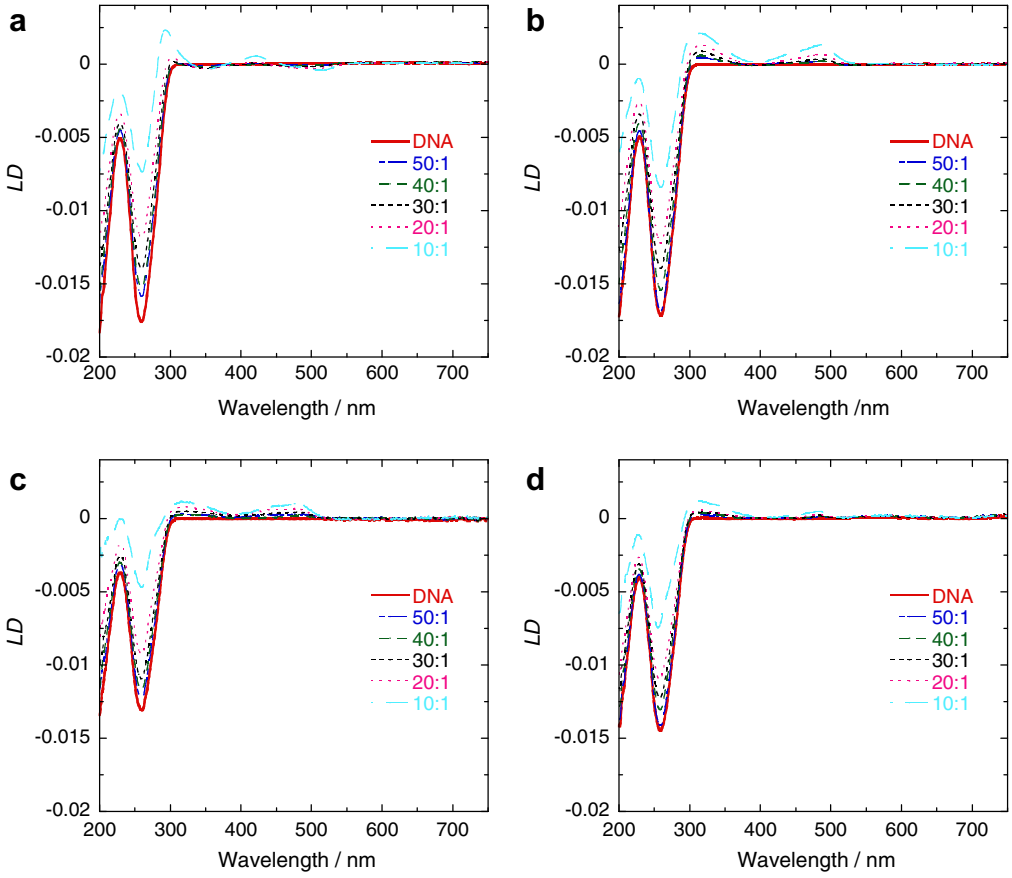

Fig. 7. LD spectra for ct-DNA (200 μM) with (a) (P)-$[Ru_2(bpy)_4L^1]^{4+}$, (b) (M)-$[Ru_2(bpy)_4L^1]^{4+}$, (c) (P)-$[Ru_2(phen)_4L^1]^{4+}$ and (d) (M)-$[Ru_2(phen)_4L^1]^{4+}$. Mixing ratios are indicated in each figure. All spectra were run in 50 mM NaCl and 1 mM sodium cacodylate buffer with 18.2 MΩ water. The cell path length was 1 mm.

The (M)-bpy and (P)-phen complexes have a comparatively large positive LD in both MLCT and in-ligand regions. The (P)-bpy and (M)-phen complexes show little complex orientation until high loading and what there is gives a negative/positive MLCT LD pattern for (P)-bpy and positive only for (M)-phen. Thus, as with the ICD, (P)-bpy is different from the others. Film LD has shown that the long wavelength MLCT bands of both complexes (440–480 nm) are predominantly *x*/*y* (short axis)-polarised as are the signals at 280/270 nm, while the transitions between are a mixture of *x*/*y* and *z*-polarisations with *z* dominating [36]. The positive MLCT flow LD signals of (M)-bpy, (P)-phen and (M)-phen thus indicate that the short axis of these complexes is more parallel than perpendicular to the *average* DNA axis as is the case for both parent iron triple-helical cylinder enantiomers. The converse is the case for (P)-bpy whose *z*-axis is more parallel to the net DNA orientation axis. Unfortunately, as with $[Fe_2L^1_3]^{4+}$, since the complexes are bending the DNA we cannot use the average base LD signal as an indication of DNA orientation in the region of the binding site.

In order to determine whether there was any sequence dependence of the DNA binding and bending of the complexes, LD spectra with GC and AT-DNA were measured. Due to the differences in polymer chain length, and hence the orientation parameter, ct-DNA gives the largest signal intensity at approximately 260 nm. However, despite the smaller magnitude signals, it is apparent that AT and GC both lose LD intensity upon addition of the ruthenium complexes (Supplementary information, Figures S5 and S6) in a manner that is proportional to the concentration of added ruthenium. There is no evidence of an oriented MLCT band with any of the complexes except (P)-phen with AT (which is positive). However, a small difference between the DNA and DNA plus complex could be hidden in the noise levels of the signal. The variation in DNA loss of orientation as a function of sequence and complex is marked. The bpy complexes, especially (P)-bpy, bend AT much more than GC with ct-DNA being in the middle. This might be attributed only to the greater flexibility of AT-DNA. (P)-phen, by way of contrast, bends GC more than AT, whereas (M)-phen dramatically bends AT. These observations suggest sequence specific interactions. The phen compounds have more effect on the alternating homopolymers than on the random sequence ct-DNA. The diastereomeric mixtures are effective at bending the homopolymeric DNA in contrast to the situation with ct-DNA.

4. Gel electrophoresis

A complementary probe of ligand effects on DNA structure that allows size change of DNA to be probed is to determine how the gel mobility of negatively supercoiled plasmids is affected. If the ligand unwinds DNA, as for example an intercalator does, the supercoiled plasmid unwinds until there is a point where the loading is such that it comigrates with free open circle DNA. For groove-binders, the effect depends on how the ligand binds and the mechanism by which it unwinds or otherwise affects the DNA structure.

In the gel electrophoresis experiments of this work, an agarose gel was loaded with plasmid pBR322 DNA and plasmid DNA plus different ruthenium complex concentrations. The plasmid DNA is mainly negatively supercoiled but has a small concentration of open circle DNA. The supercoiled plasmid is more compact than the open circle DNA and thus runs more quickly. In our experiments (Fig. 5, note ratios of gels are in terms of DNA base pairs), it is immediately apparent that the unwinding effects are not particularly dramatic. As a control, gels of (M)-, rac-, and (P)-$[Fe_2L^1_3]^{4+}$ were also performed (Supplementary information, Figure S6). Thus, of the bpy compounds only M-bpy induces any DNA unwinding, but even at very high loading the bands do not comigrate indicating that the unwinding effect is small (<5°). Some unwinding is also observed for the M and P phen enantiomers. Thus, the DNA is becoming somewhat longer and/or stiffer with (M)-bpy, (P)-phen and (M)-phen. As the loss of LD signal (see Fig. 7, Table 1 for summary) for all complexes requires the DNA to be either being bent or becoming more flexible (so less well oriented), we can, therefore, conclude that (M)-bpy, (P)-phen and (M)-phen all bend and stiffen DNA. The loss of DNA LD with (P)-bpy, the appearance of an in-ligand LD signal at high loading, yet its constant gel mobility as a function of loading argues for a regular rigid but compact structure. The results also show a decrease in the efficiency of the ethidium bromide staining with complex loading reflecting the fact that the ruthenium complexes bind more strongly to DNA so the EB is unable to displace the ruthenium complex. The gels also shows changes to the relaxed DNA mobility upon ruthenium binding at higher concentrations which may indicate a slight shortening or condensing effect on the DNA structure (Fig. 8).

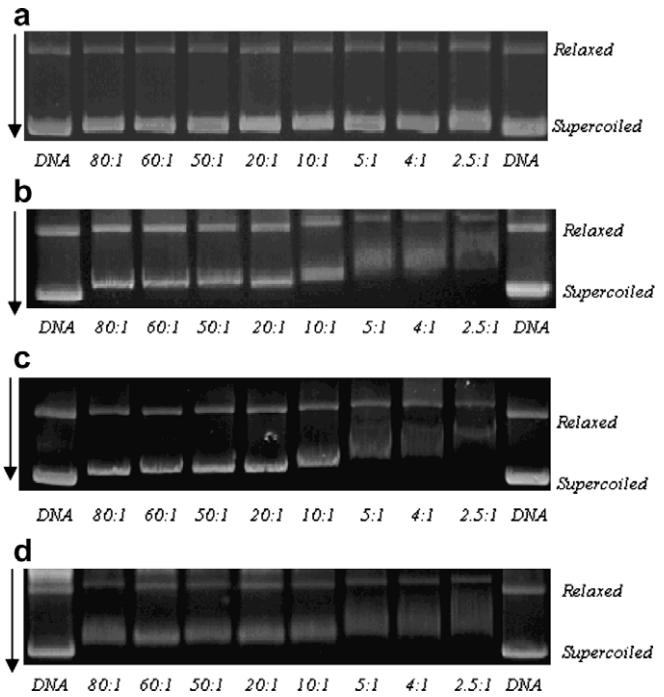

Fig. 8. Agarose gel (1.0%) of pBR322 plasmid DNA (48 μM DNA in basepairs) treated with (a) (P)-$[Ru_2(bpy)_4L^1]^{4+}$, (b) (M)-$[Ru_2(bpy)_4L^1]^{4+}$, (c) (P)-$[Ru_2(phen)_4L^1]^{4+}$ and (d) (M)-$[Ru_2(phen)_4L^1]^{4+}$ from left to right, 0, 0.6, 0.8, 0.9, 2.4, 4.8, 9.6, 12.0, 19.3 and 0 μM. Arrow depicts migration direction.

5. Conclusions

Absorbance, circular dichroism, fluorescence displacement, DNA melting, linear dichroism spectroscopy and gel electrophoresis have been used to probe the binding of the enantiomers of two bimetallo ruthenium complexes to DNA. All complexes bind to DNA strongly enough for all of the complex present in any of the experiments to be treated as bound to DNA. Our expectation from the literature [12,23,47–51] was that the bpy complexes would bind more weakly than the phen ($[Ru(bpy)_3]^{2+}$ has been shown to have $K_a \sim 10^3\,M^{-1}$ at 50 mM ionic strength[9]) and probably mainly via external electrostatic interactions. The bpy complexes do indeed bind less strongly than the phen, though not significantly so. The binding constants range from $10^6\,M^{-1}$ for the weakest ruthenium bipyridine complexes to $10^7\,M^{-1}$ for the strongest ruthenium phenanthroline complexes. Within each series the binding strength order is: (M) > diastereomeric mixture > (P). All

complexes also bend the DNA. The complexes then separate into two groups: (P)-bpy behaves quite differently from the others.

(P)-bpy has identical ICD signals at all ratios so is not interacting closely with the DNA bases. Its LD is consistent with its *z*-axis being close to along the DNA orientation axis in contrast to all other dimetallo helicate-type complexes we have studied [30,31,46]. It also bends AT most which is consistent with the flexibility of such sequences (and contrasts the effect of (P)-phen). However, despite the loss of DNA orientation, at high loading, the (P)-bpy/AT complex has a positive in-ligand region (*z*-polarised) LD signal. In addition, despite the changes in LD intensity, the gel mobility of plasmid DNA is unaffected by (P)-bpy. Further, (P)-bpy is the most effective of the bpy complexes at stabilising the duplex DNA yet it is also the weakest binder. All of this combines to suggest that (P)-bpy forms a regular rigid but compact structure of the DNA. One option would be for (P)-$[Ru_2(bpy)_4L^1]^{4+}$ to bind externally perhaps with chelates spanning a groove, similar to the mode proposed for (P)-$[Ru(phen)_3]^{2+}$ [23], but without the middle aromatic ring of the chelate slotted into the groove. It could then induce a type of supercoiling of the DNA about itself like ribbon round a pole of helicates. This would certainly be an effective method of stabilising the DNA duplex and is consistent with the other observations.

Our data lead us to conclude that (M)-bpy, (P)-phen and (M)-phen interact with the bases in sequence selective modes and bend and stiffen the DNAs with a net reduction in orientation. (P)-phen has most bending effect on GC which is unusual given the greater stability of the G≡C base pair compared with the A=T pair, so the mode adopted with GC must favour bending. (P)-phen and (M)-bpy have larger positive MLCT LD signals than (M)-phen, though all bend DNA similarly. Thus, (P)-phen has its *x*/*y* plane closer to the average DNA axis than (M)-phen and thus its *z*-axes across the DNA orientation axis as is the case for $[Fe_2L^1_3]^{4+}$ [31]. It is tempting to conclude, given this and the matching of the signs of the phen enantiomers' ICD with that of the $[Fe_2L^1_3]^{4+}$ enantiomers [31], that (M)-phen is a major-groove binder and (P)-phen a major/minor groove binder as we suspect is the case for $[Fe_2L^1_3]^{4+}$. However, the evidence for this tidy conclusion is far from conclusive. The variation in DNA loss of orientation as a function of sequence and complex is marked. (P)-phen bends GC more than AT, whereas (M)-phen dramatically bends AT. This suggests (P)-phen dominates the binding to GC and (M)-phen to AT.

The diruthenium complexes of this work structurally may be viewed either as two bis(bipyridine) or bis(phenanthroline) monoruthenium complexes held together by a linking ligand, or as a more enantiomerically stable and presumably more flexible analogue of the di-iron triple-helical cylinder of Fig. 1. The results show that the metal complexes bind orders of magnitude more strongly to DNA than the mononuclear complexes and only slightly less strongly than the di-iron cylinder ($[Fe_2L^1_3]^{4+}$). In other respects, however, the (P)-bpy behaves analogously to the mononuclear complex whereas (M)-bpy seems to be a groove binder that bends the DNA. The DNA binding behaviour of the phen complexes is entirely consistent with that of the di-iron helicates in terms of the induced CD signals and DNA bending effects and so does not behave as close-packed mononuclear complexes. Thus, the phen complexes provide a chemically and enantiomerically stable alternative to the DNA-coiling di-iron triple helical cylinder previously studied—though aspects of the di-iron cylinder DNA binding are driven by its symmetry such as the formation of the three-way junction [32] are not expected.

6. Abbreviations

bpy	2,2′-bipyridine
CD	circular dichroism
ct-DNA	calf thymus DNA
DNA	deoxyribonucleic acid
EB	ethidium bromide
ICD	induced CD
L^1	bis(pyridylimine) ligand ($(C_5H_4N)C{=}N(C_6H_4))_2CH_2$)
LD	linear dichroism
M	minus
MLCT	metal ligand charge transfer
P	plus
phen	1,10-phenanthroline
T_m	melting temperature
vis	visible

Acknowledgements

Dr. Jaroslav Malina and Carlos Sanchez-Cano are thanked for helpful comments on the experimental data. U.M. and M.R.H. acknowledge funding from the EPSRC.

Supplementary data

Supplementary data associated with this article can be found, in the online version, at doi:10.1016/j.jinorgbio.2008.06.006.

References

[1] A. Juris, V. Balzani, P. Belser, A. Von Zelewsky, Helvetica Chim. Acta 64 (1981) 2175–2182.
[2] V. Balzani, A. Juris, M. Venturi, S. Campagna, S. Serroni, Chem. Rev. 96 (1996) 759–833.
[3] K. Kalyanasundaram, Coord. Chem. Rev. 46 (1982) 159.
[4] E. Krausz, H. Risen, Coord. Chem. Rev. 159 (1997) 9.
[5] Y. Xiong, L.N. Ji, Coord. Chem. Rev. 185–186 (1999) 711–733.
[6] G.I. Pascu, A. C.G. Hotze, C. Sanchez Cano, B.M. Kariuki, M.J. Hannon, Angew. Chem., Intl. Ed. 46 (2007) 4374–4378.
[7] M.J. Hannon, Chem. Soc. Rev. 36 (2007) 280–295.
[8] A.D. Richards, A. Rodger, Chem. Soc. Rev. 36 (2007) 471–483.
[9] J.K. Barton, L.A. Basile, A. Danishefsky, A. Alexandrescu, Proc. Natl. Acad. Sci. USA 81 (1984) 1961–1965.
[10] C. Metcalfe, J.A. Thomas, Chem. Soc. Rev. 32 (2003) 215–224.
[11] C. Hiort, B. Nordén, A. Rodger, J. Am. Chem. Soc. 112 (1990) 1971–1982.
[12] C. Hiort, P. Lincoln, B. Nordén, J. Am. Chem. Soc. 115 (1993) 3448–3454.
[13] B.T. Patterson, J.G. Collins, F.M. Foley, F.R. Keene, Dalton Trans. (2002) 4343–4350.
[14] A.H. Velders, H. Kooijman, A.L. Spek, J.G. Haasnoot, D. de Vos, J. Reedijk, Inorg. Chem. 39 (2000) 2966–2967.
[15] V. Brabec, J. Kasparkova, Drug Resistance Updates 8 (2005) 131–146.
[16] M.J. Hannon, Pure Appl. Chem. 79 (2007) 2243–2261.
[17] M. Clarke, F. Zhu, D.R. Frasca, Chem. Rev. 99 (1999) 2511–2533.
[18] W.H. Ang, P.J. Dyson, Eur. J. Inorg. Chem. (2006) 4003–4018.
[19] U.K. Mazumder, M. Gupta, S.S. Karki, S. Battacharya, S. Rathinasamy, T. Sivakumar, Bioorg. Med. Chem. 13 (2005) 5766–5773.
[20] P. Schluga, C. Hartinger, A. Egger, E. Reisner, M. Galanski, M.A. Jakupec, B.K. Keppler, Dalton Trans. (2006) 1796–1802.
[21] C. Kumar, J.K. Barton, N.J. Turro, J. Am. Chem. Soc. 107 (1985) 5518–5523.
[22] I.S. Haworth, A.H. Elcock, J. Freeman, A. Rodger, W.G. Richards, J. Biomol. Struct. Dyn. 9 (1991) 23–44.
[23] D.Z.M. Coggan, I.S. Haworth, P.J. Bates, A. Robinson, A. Rodger, Inorg. Chem. 38 (1999) 4486–4497.
[24] M. Eriksson, M. Leijon, C. Hiort, B. Nordén, A. Graslund, Biochemistry 33 (1994) 5031–5040.
[25] J.P. Rehmann, J.K. Barton, Biochemistry (1990) 1701.
[26] J. Aldrich-Wright, C. Brodie, E.C. Glazer, N.W. Luedtke, L. Elson-Schwab, Y. Tor, Chem. Commun. (2004) 1018–1019.
[27] F. Westerlund, M. Wilhelmsson, B. Nordén, P. Lincoln, J. Phys. Chem. B 109 (2005) 21140–21144.
[28] B. Onfelt, P. Lincoln, B. Nordén, J. Am. Chem. Soc. 123 (2001) 3630–3637.
[29] J.A. Smith, J.G. Collins, B.T. Patterson, F.R. Keene, Dalton Trans. (2004) 1277–1283.
[30] M.J. Hannon, V. Moreno, M.J. Prieto, E. Moldrheim, E. Sletten, I. Meistermann, C.J. Isaac, K.J. Sanders, A. Rodger, Angew. Chem., Intl. Ed. 113 (2001) 904–908.
[31] I. Meistermann, V. Moreno, M.J. Prieto, E. Moldrheim, E. Sletten, S. Khalid, P.M. Rodger, J.C. Peberdy, C.J. Isaac, A. Rodger, M.J. Hannon, Proc. Natl. Acad. Sci. USA 99 (2002) 5069–5074.
[32] A. Oleksi, A.G. Blanco, R. Boer, I. Usón, J. Aymamí, A. Rodger, M.J. Hannon, M. Coll, Angew. Chem. Intl. Ed. 45 (2006) 1227–1231.
[33] L. Cerasino, M.J. Hannon, E. Sletten, Inorg. Chem. 46 (2007) 6245–6251.

[34] J. Malina, M.J. Hannon, V. Brabec, Chem. – A. Eur. J. 13 (2007) 3871–3877.
[35] L.J. Childs, J. Malina, B.E. Rolfsnes, M. Pascu, M.J. Prieto, M.J. Broome, P.M. Rodger, E. Sletten, V. Moreno, A. Rodger, M.J. Hannon, Chem. – A Eur. J. 12 (2006) 4919–4927.
[36] S. Khalid, M.J. Hannon, A. Rodger, P.M. Rodger, Chem. – A Eur. J. 12 (2006) 3493–3506.
[37] C. Uerpmann, J. Malina, M. Pascu, G.J. Clarkson, V. Moreno, A. Rodger, A. Grandas, M.J. Hannon, Chem. Eur. J. 11 (2005) 1750–1756.
[38] U. McDonnell, J.M.C.A. Kerchoffs, R.P.M. Castineiras, M.R. Hicks, M. A.C.G. Hotze, M.J. Hannon, A. Rodger, Dalton (2008) 667–675.
[39] S. Khalid, P.M. Rodger, A. Rodger, J. Liq. Chromat. 28 (2005) 2995–3003.
[40] M.J. Hannon, C.L. Painting, A. Jackson, J. Hamblin, W. Errington, Chem. Comm. (Cambridge) (1997) 1807–1808.
[41] J.C.M.A. Kerckhoffs, J.C. Peberdy, I. Meistermann, L.J. Childs, C.J. Isaac, C.R. Pearmund, V. Reudegger, N.W. Alcock, M.J. Hannon, A. Rodger, Dalton Trans. (2007) 734–742.
[42] A. Rodger, in: J.F. Riordan, B.L. Vallee (Eds.), Methods in Enzymology, vol. 226, Academic Press, San Diego, 1993, pp. 232–258.
[43] J. Sambrook, E.F. Fritsch, T. Maniatis, Molecular Cloning: A Laboratory Manual, Cold Sping Harbor Laboratory Press, New York, 1989.
[44] C. Hiort, P. Lincoln, B. Nordén, J. Am. Chem. Soc. 115 (1993) 3448–3454.
[45] C.Y. Zhou, J. Zhao, Y.B. Wu, C.X. Yin, P. Yang, J. Inorg. Biochem. 101 (2007) 10–18.
[46] J.C. Peberdy, J. Malina, S. Khalid, M.J. Hannon, A. Rodger, J. Inorg. Biochem. 101 (2007) 1937–1945.
[47] H. Görner, A.B. Tossi, C. Stradowski, D. Schulte-Frohlinde, J. Photochem. Photobiol. B 2 (1988) 67–89.
[48] T. Härd, B. Nordén, Biopolymers 25 (1986) 1209–1228.
[49] K.A. O'Donoghue, J.M. Kelly, P.E. Kruger, Dalton Trans. (2004) 13–15.
[50] A.M. Pyle, J.P. Rehmann, R. Meshoyrer, C.V. Kumar, N.J. Turro, J.K. Barton, J. Am. Chem. Soc. 111 (1989) 3051–3058.
[51] F.M. O'Reilly, J.M. Kelly, J. Phys. Chem. B 104 (2000) 7206–7213.